The phonon density of states and low-temperature specific heat: the blue bronze $K_{0.3}MoO_3$ and the platinum chain compound KCP



1997 J. Phys.: Condens. Matter 9 8639

(http://iopscience.iop.org/0953-8984/9/41/011)

J. Phys.: Condens. Matter **9** (1997) 8639–8655. Printed in the UK PII: S0953-8984(97)84875-8

# The phonon density of states and low-temperature specific heat: the blue bronze $K_{0.3}MoO_3$ and the platinum chain compound KCP

H Requardt†‡, R Currat†, P Monceau‡, J E Lorenzo§, A J Dianoux†, J C Lasjaunias‡ and J Marcus‖

† Institut Laue–Langevin, 38042 Grenoble, France
‡ Centre de Recherches sur les Très Basses Températures, CNRS, 38042 Grenoble, France
§ Laboratoire de Cristallographie, CNRS, 38042 Grenoble, France
‖ Laboratoire d'Etudes des Propriétés Electroniques des Solides, CNRS, 38042 Grenoble, France

Received 2 June 1997

**Abstract.** The quasi-one-dimensional charge-density-wave (CDW) compounds $(TaSe_4)_2I$, the blue bronze $K_{0.3}MoO_3$ and the platinum chain compound KCP(Br) show a strong deviation from a Debye behaviour of the specific heat $C_P$ at temperatures of several degrees Kelvin. To determine the origin of this specific heat 'anomaly' in the case of $K_{0.3}MoO_3$, we have performed time-of-flight neutron scattering measurements and extracted a generalized phonon density of states (PDOS). The excess over a Debye behaviour at low energies in the generalized PDOS lies at the origin of the observed anomalous specific heat. We have used a simplified dispersion model based on experimental phonon dispersion curves to calculate the low-energy PDOS of the system. The model succeeds in reproducing the observed specific heat anomaly and establishes its lattice phonon origin. Similar calculations of the low-energy PDOS based on available phonon dispersion data for KCP allow us to state that the anomalous behaviour of the specific heat for this compound also has a phonon origin.

## 1. Introduction

Many quasi-one-dimensional compounds like $NbSe_3$, $(TaSe_4)_2I$, $K_{0.3}MoO_3$, and KCP ($K_2[Pt(CN)_4]X_{0.3}\cdot 3.2\ H_2O$, X = Br, Cl) undergo a Peierls transition into a state of modulated electron density, the charge-density wave (CDW), and a periodic distortion of the parent lattice. The corresponding modulation wavenumber is $q = 2k_F$, where $k_F$ is the Fermi wavenumber [1, 2]. A characteristic feature of CDW systems is the very pronounced phonon softening (Kohn anomaly) at around the modulation wave vector $q$. This has been observed in $K_{0.3}MoO_3$ [3, 4] and KCP [5], whereas no Kohn anomaly has been observed in $(TaSe_4)_2I$ [6].

For some of the CDW compounds, $(TaSe_4)_2I$ [7], $A_{0.3}MoO_3$ (A = K, Rb) [8, 9] and KCP [10], measurements of the specific heat $C_P$ have revealed a pronounced deviation from a Debye-like behaviour, observable as a bump in $C_P/T^3$ centred around temperatures between 1.8 K and about 12 K for $(TaSe_4)_2I$ and $K_{0.3}MoO_3$, respectively. The anomalous behaviour which has been observed in $(TaSe_4)_2I$ (see figure 1), was firstly ascribed to excitations of pinned phason modes of the CDW. This interpretation was suggested by the fact that this specific heat behaviour is observed in the CDW system $(TaSe_4)_2I$, but not in the structurally related, *non*-CDW system $(NbSe_4)_3I$ [7]. In addition, the energy range

0953-8984/97/418639+17$19.50  

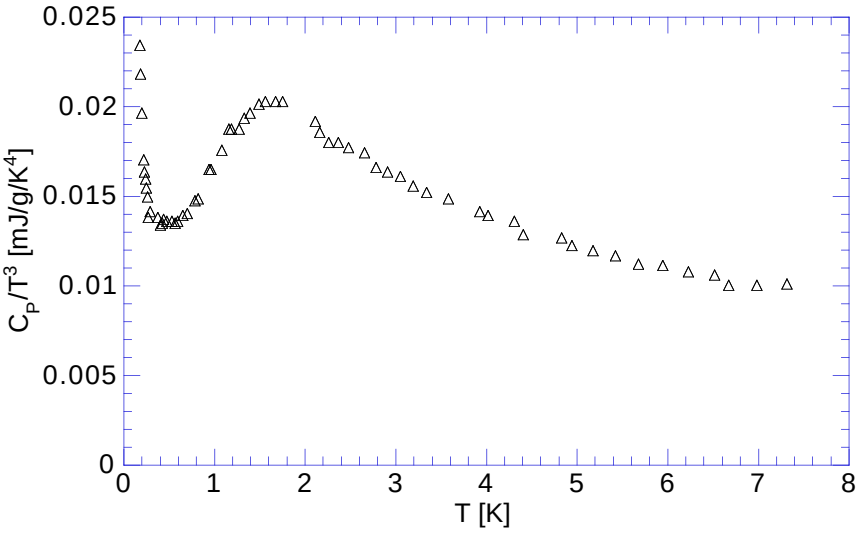


**Figure 1.** The low-temperature specific heat of $(TaSe_4)_2I$. The data are taken from [7].

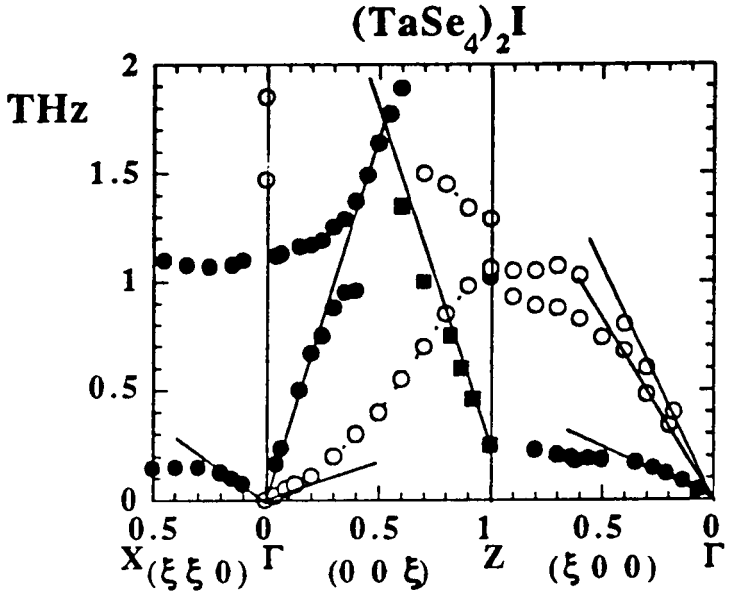


**Figure 2.** The low-frequency phonon branches of $(TaSe_4)_2I$. (This figure is taken from [18].) Modes polarized parallel to the chain direction are shown as full symbols, modes perpendicular to the chains as open symbols. The corresponding sound velocities are indicated as lines.

of the pinned phasons in $(TaSe_4)_2I$, 0.2–1.1 meV (1 meV = 0.242 THz = 8.065 cm$^{-1}$), deduced from ac-conductivity [11, 12] and neutron scattering experiments [13], corresponds well to the temperature (1.8 K) of this specific heat 'anomaly'.

The phason interpretation was later questioned as a result of $C_P$-experiments on Nb-doped $(TaSe_4)_2I$ samples [14] indicating a persisting anomalous specific heat behaviour

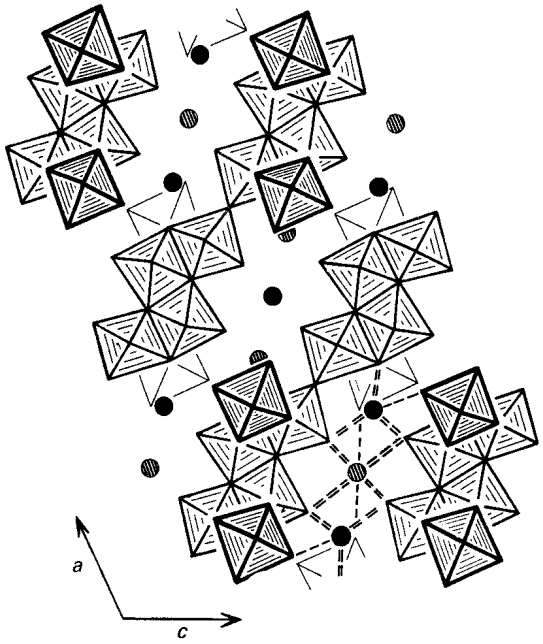


**Figure 3.** The sheet-like structure of $K_{0.3}MoO_3$: planes of $MoO_6$ octahedra separated by the potassium ions. The projection is along the chain direction [0, 1, 0]. The potassium ions are positioned at two levels: $y = 0$ (hatched circles) and $y = \frac{1}{2}$ (full circles). (This figure is taken from [20].)

with the maximum of the bump at the same temperature as for the pure compound. As ac-conductivity measurements on the Nb-doped compounds [15] show a shift of the pinned phason mode to higher frequencies, the interpretation of the anomaly in terms of phason excitations is questionable. Furthermore, similar behaviour of the specific heat is not observed for other CDW systems such as $NbSe_3$ [16] and $TaS_3$ [17].

Lorenzo *et al* [18] have recently related the specific heat anomaly at 1.8 K of $(TaSe_4)_2I$ to an excess of the low-energy phonon density of states (PDOS) at energies around 0.7 meV. This excess in the PDOS originates from the particular, one-dimensional character of the low-energy phonon branches, especially from a nearly dispersionless transverse acoustic phonon branch polarized along the chains and propagating in the plane perpendicular to the quasi-one-dimensional direction (see figure 2).

The specific heat 'anomalies' of the compounds $K_{0.3}MoO_3$ and KCP appear at rather high temperatures (around $T = 12$ K for the blue bronze and around 7.5 K for the platinum compound), corresponding to energies of about 6 meV and 3.5 meV, respectively. It seems unlikely that the phason interpretation holds in these cases, since the energies related to the pinned phasons are in a range below 2 meV: for $K_{0.3}MoO_3$ Degiorgi *et al* [19] have found by ac-conductivity measurements that the phason gap is at about 0.4 meV; for KCP the Kohn anomaly has been observed in neutron scattering experiments at energies down to below 1.5 meV [5] (compare figure 11, later).

In fact, the anomalous specific heat of the blue bronze compound has been ascribed to a phonon origin by Konate [8]. It is interpreted as coming from an Einstein mode at an energy $\omega \approx 4.3$ meV (35 $cm^{-1}$) and related to optical vibrations of the K ions in the compound. This interpretation is unlikely to hold, since comparison with the dispersion

curves now available (reference [3]; see figure 9, later) does not reveal an Einstein-like mode at this low energy, and the lowest optic mode has been observed at about 8 meV.

The purpose of the present study is to discover the origin of the low-temperature specific heat, deviating from a simple $T^3$-behaviour, of the blue bronze $K_{0.3}MoO_3$ and the platinum chain compound KCP.

The monoclinic system blue bronze $K_{0.3}MoO_3$ (space group $C2/m$) shows a structure in the form of infinite sheets of $MoO_6$ octahedra separated by potassium ions, as shown in figure 3. It undergoes a Peierls transition at a transition temperature $T_P = 183$ K and develops an incommensurate lattice modulation with wave vector $(1, 2k_F, 0.5)$, with $\boldsymbol{b}^*$ the chain direction [21]. The specific heat curve $C_P(T)$ of $K_{0.3}MoO_3$ has been measured up to 25 K by Odin *et al* [9]. It reveals a very broad deviation of the specific heat from a Debye behaviour, with a maximum of $C_P/T^3$ at 12 K (figure 4).

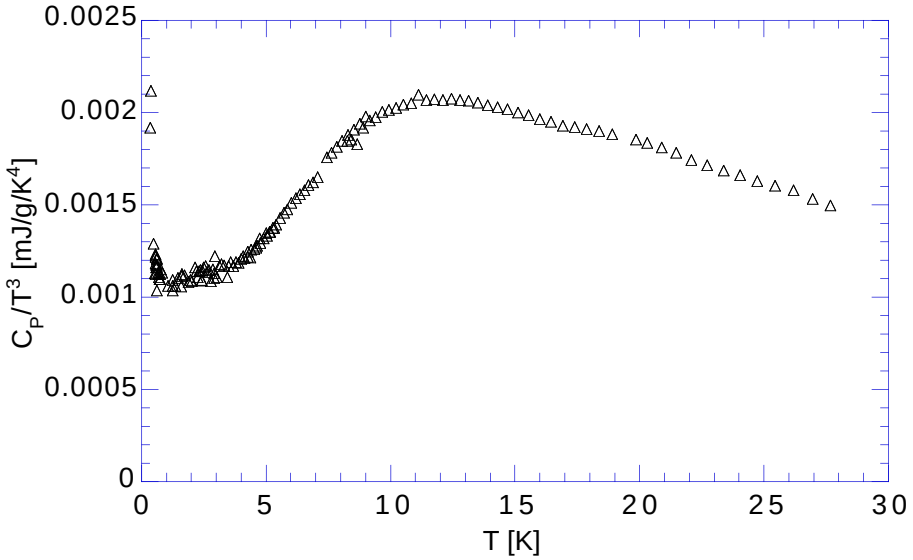


**Figure 4.** The specific heat $C_P/T^3$ of $K_{0.3}MoO_3$ for temperatures between 0.5 K and 25 K, showing a large bump with a maximum at around 12 K. The data are taken from [9].

We have carried out time-of-flight neutron scattering measurements, from which a generalized phonon density of states was deduced in order to study the phonon contribution to the specific heat below 25 K. On the basis of phonon dispersion curves measured by Pouget *et al* [3] (figure 9—see later), we have constructed a simplified dispersion model (see section 3.2) and calculated the low-energy PDOS. Comparison of the experimental and the calculated PDOS, and the calculation of the corresponding specific heat have allowed us to relate the observed specific heat behaviour to particular phonon branches.

The platinum chain compound KCP shows a tetragonal structure (space group $P4mm$) made up of infinite chains of $Pt(CN)_4$ groups separated by the potassium cations and the halogen (Br, Cl) anions (figure 5). For KCP bromide (KCP(Br)) the Peierls temperature is about 100 K and the incommensurate modulation wave vector is $(\frac{1}{2}a^*, \frac{1}{2}a^*, 2k_F)$ with $2k_F \approx 0.3c^*$ and with $\boldsymbol{c}^*$ along the chain direction [22]. For deuterated KCP(Br), Odin *et al* [10] have measured the specific heat curve between about 2 K and 30 K, revealing a deviation from a simple $T^3$-law with a maximum at around 7.5 K (figure 6). To determine the origin of this specific heat behaviour, we have used low-energy phonon dispersion curves

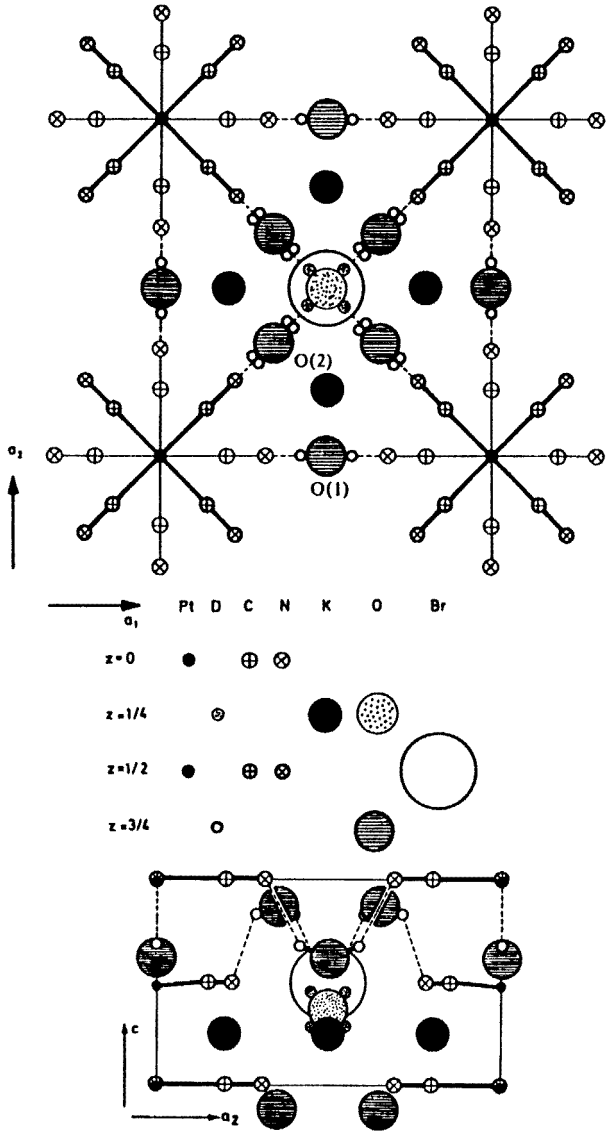


**Figure 5.** The crystal structure of deuterated KCP(Br) ($K_2[Pt(CN)_4]Br_{0.3}\cdot 3.2\,D_2O$). Upper part: projection along the tetragonal $c^*$-axis. Lower part: projection along one $a^*$-axis. (This figure is from [23].)

measured by Carneiro *et al* [5] to calculate the low-energy PDOS in an approach similar to that used for $K_{0.3}MoO_3$.

## 2. Experimental procedure

The experiment was performed on the time-of-flight spectrometer IN6 at the Institut Laue–Langevin (Grenoble, France). The instrument was operated in the neutron energy-gain mode

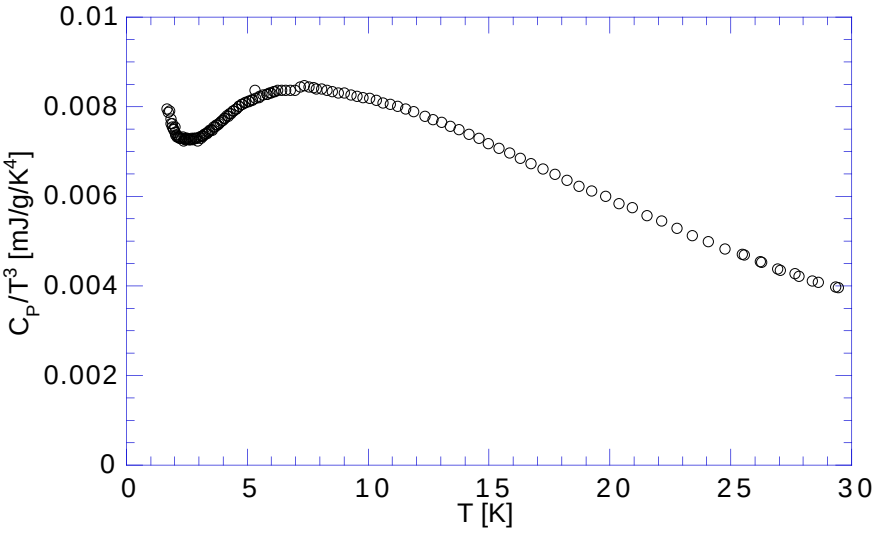


**Figure 6.** The low-temperature specific heat $C_P/T^3$ of KCP(Br) showing the deviation from a $T^3$-behaviour with the maximum at about 7 K. The data are taken from [10].

('up-scattering') using an incident neutron energy of 3.12 meV (5.12 Å). At the elastic line, the instrument offers an energy resolution of 0.1 meV. The scattered neutrons are detected with in total 337 detectors covering a range of scattering angles $2\Theta$ from $10^\circ$ up to $115^\circ$.

Measurements were carried out at several temperatures between 100 K and 450 K on a powdered sample contained in a flat, thin-walled aluminium cell. To allow us to correct the scattered signal from the sample container and the background, the runs were repeated with empty cells.

From the measured time-of-flight spectra, one calculates the scattering function $S(\Theta, \omega)$ using the equation

$$S(\Theta, \omega) = \frac{\partial^2\sigma}{\partial\Omega\,\partial t}\frac{t^4}{2t_0^3}\mathrm{e}^{-\hbar\omega/2k_BT} \tag{1}$$

where $t$ denotes the neutron time of flight, and $t_0$ the time of flight of the elastically scattered neutrons. The neutron energy gain $\hbar\omega = E(t) - E_0$, the momentum transfer $Q$ and the scattering angle $2\Theta$ are related through

$$Q^2 = A(2E_0 + \hbar\omega - 2\sqrt{E_0^2 + \hbar\omega E_0}\cos(2\Theta)) \tag{2}$$

with $A = 0.482$ meV Å$^2$. $E_0$ and $E(t)$ are the incident and the final neutron energy, respectively. Using the reduced variables $\alpha = \hbar^2Q^2/(2Mk_BT)$ (with $M$ the average atomic mass) and $\beta = \hbar\omega/k_BT$ one defines the spectral distribution $P(\alpha, \beta)$:

$$P(\alpha, \beta) = 2\beta\sinh\left(\frac{\beta}{2}\right)\frac{\tilde{S}(\alpha, \beta)}{\alpha}. \tag{3}$$

The Debye–Waller and the multiphonon corrections are performed selfconsistently on $P(\alpha, \beta)$.

At this stage one has to take into account that the compound under study is a nearly purely coherent scatterer. In this case, to calculate the phonon density of states one has to use the incoherent approximation [24], which means that the spectral distribution $P(\alpha, \beta)$

has to be averaged over the momentum transfer $Q$. The validity of this method rests on the assumption that the $Q$-averaged coherent cross section approximates the incoherent cross section. At large energy transfers this should be the case, since the related momentum transfers are also large (see equation (2)). In this case the combined effects of powder averaging and detector (or $Q$-) averaging guarantees the validity of this approximation.

For low energy transfers the $Q$-volume to average is quite sensitive to the incident neutron energy $E_0$ and the angular range of the detectors. The ratio between the averaging $Q$-volume and the volume of the Brillouin zone of the sample determines the applicability of the incoherent approximation. In our experiment, with a sample unit-cell volume well in the range of $10^3$ Å$^3$, the number of Brillouin zones over which it is averaged is in the range of several hundreds. This should ensure a sufficient statistical averaging of the coherent scattering cross section.

For the phonon density of states $G(\omega)$ obtained through the procedure described above, we have finally also to take into account that in a polyatomic system the scattered signal of each kind $i$ of atom (with atomic mass $m_i$) depends not only on their chemical proportion $c_i$ in the compound but also on the respective scattering cross section $\sigma_i$. So in fact we obtained a generalized or neutron-weighted phonon density of states, defined as

$$G(\omega) = \left(\sum_{i=1}^{n}(c_i\sigma_i/m_i)g_i(\omega)\right)\Big/(\sigma/M) \tag{4}$$

where $n$ is the number of different kinds of atom in the compound. $\sigma$ and $M$ are the molecular scattering cross section and the molecular mass, respectively. The $g_i(\omega)$ are the partial densities of states corresponding to the species $i$. The weighting factors for the blue bronze $K_{0.3}MoO_3$ are illustrated in the table 1. They show that more than 90% of the measured density of states originates from the oxygen atoms due to their relative abundance and the favourable ratio $\sigma_O/m_O$.

**Table 1.** The coherent scattering cross sections $\sigma_i$, atomic masses $m_i$, scattering weights $\sigma_i/m_i$ and relative scattering weight factors of K, Mo and O.

| | $\sigma_i$ (b) | $m_i$ (au) | $\sigma_i/m_i$ | $c_i$ | $c_i(\sigma_i/m_i)$ | |
|---|---|---|---|---|---|---|
| K | 1.73 | 39.1 | 0.044 25 | 6.98% | 0.0031 | 1.52% |
| Mo | 6.07 | 95.94 | 0.063 27 | 23.26% | 0.0147 | 7.27% |
| O | 4.235 | 16.0 | 0.2647 | 69.77% | 0.1847 | 91.21% |

## 3. Results and discussion

### *3.1. $K_{0.3}MoO_3$: the experimental phonon density of states and low-temperature specific heat*

Figure 7 shows the generalized phonon density of states resulting from the data analysis described above for several temperatures above and below the phase transition temperature. The PDOS profiles reveal a large number of features with changes in amplitude but no variation of the energy for the different temperatures. This may arise from an anisotropic Debye–Waller factor, changing its anisotropy with temperature. During the data treatment the Debye–Waller factor is taken to be isotropic, a simplification for rather two-dimensional structures like the blue bronze (see figure 3). This leads to an artificial enhancement or depression of phonon branches depending on their polarization.

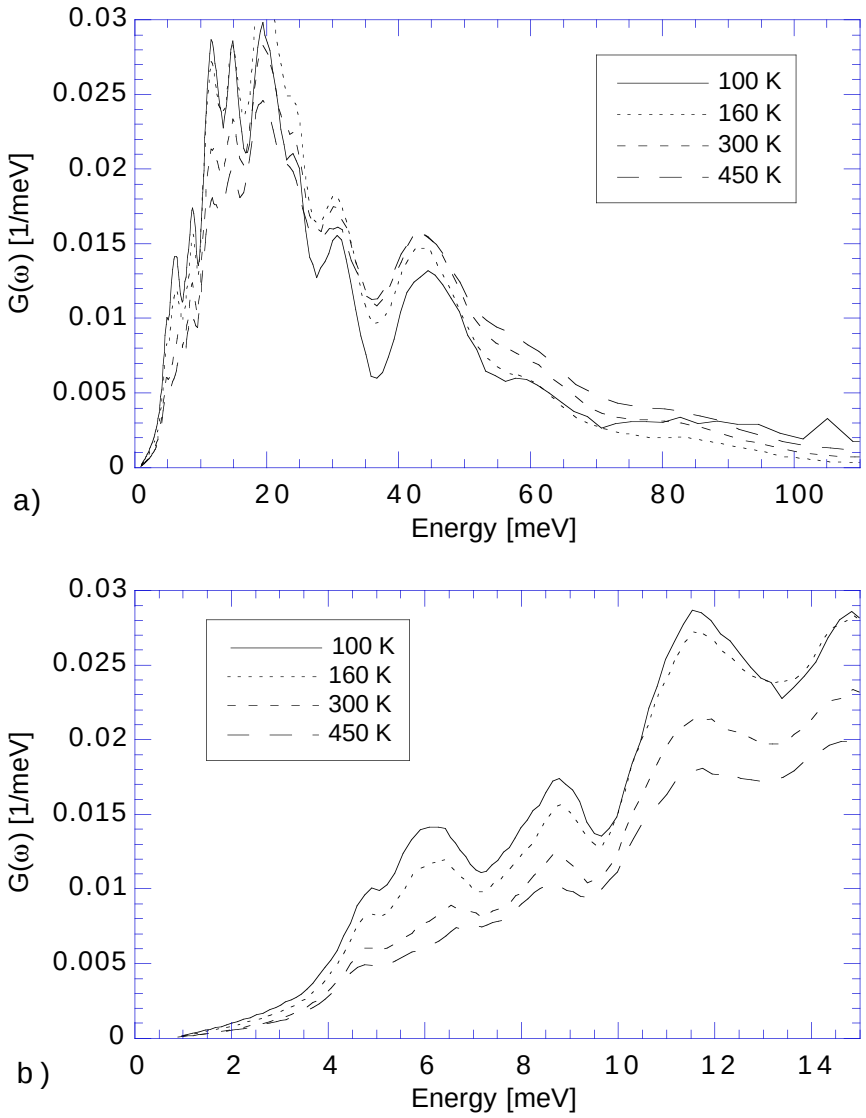


**Figure 7.** The experimental (generalized) phonon density of states (PDOS) of the blue bronze $K_{0.3}MoO_3$ at several temperatures. (a) The energy spectrum up to the cut-off (≈110 meV, taken from reflectivity data from [19]); (b) the low-energy part. Each of the PDOSs is normalized to unit area.

The PDOS data are used to calculate the specific heat $C_P$:

$$C_P(T) = 3n\frac{R}{M}\int x^2 \frac{\exp(x)}{(\exp(x)-1)^2} G(\omega)\ \mathrm{d}\omega \tag{5}$$

with $x = \hbar\omega/k_BT$ and $R = 8.314$ J mol$^{-1}$ K$^{-1}$ the molar gas constant. $G(\omega)$ is the PDOS, normalized to unit area via $\int G(\omega)\ \mathrm{d}\omega = 1$. $M$ is the molar mass of a unit cell and $n$ the number of atoms per unit cell ($M = 1557$ g mol$^{-1}$, $n = 43$ for $K_{0.3}MoO_3$ and $M = 465$ g mol$^{-1}$, $n = 21$ for deuterated KCP(Br)). In this equation no adjustable parameter is involved.

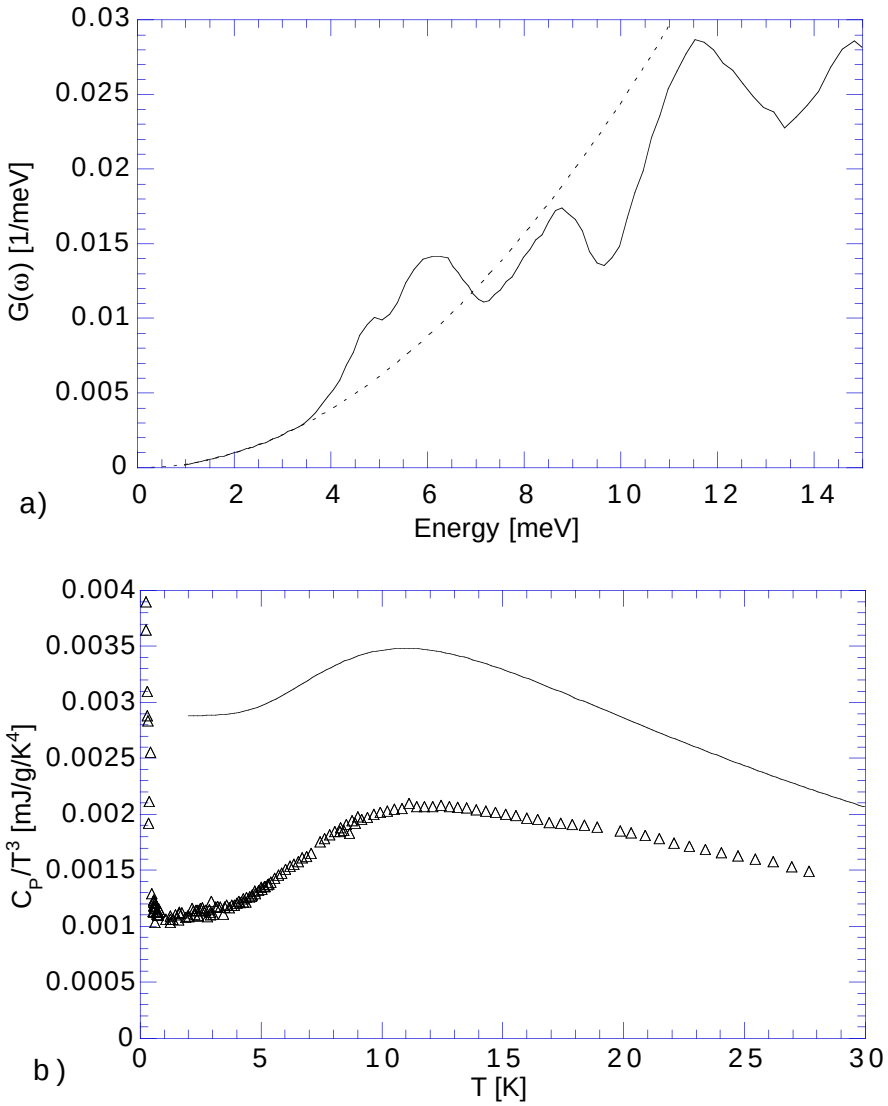


**Figure 8.** (a) The low-energy generalized PDOS of $K_{0.3}MoO_3$ at $T = 100$ K. The dashed line extrapolates a Debye law fitted to the generalized PDOS (full line) below 3 meV to show the excess of the PDOS over a Debye behaviour. (b) The specific heat $C_P/T^3$ (full line) calculated from the generalized PDOS. The experimental specific heat data are plotted as symbols.

Since phonon contributions at energies higher than 15 meV contribute only negligibly to the specific heat at temperatures up to 12 K, we will concentrate the discussion on this low-energy range (see figures 7(b) and 8(a)). The principal features of the low-energy PDOS are the following:

(1) a Debye-like behaviour up to about 3 meV; and

(2) when extrapolating a parabolic fit $a\omega^2$ (for the Debye part) to higher energies, the PDOS between 4 meV and about 7 meV exceeds a Debye behaviour (figure 8(a)).

When calculating the specific heat from the generalized PDOS, one obtains a behaviour

of $C_P/T^3$ as shown in figure 8(b). It reveals qualitatively the same behaviour as the measured specific heat:

(1) a flat part, the 'Debye plateau', below about 4 K, corresponding to a pure Debye behaviour in this temperature range, which means a Debye behaviour in the lowest few meV of the PDOS; and

(2) a bump in $C_P/T^3$ for temperatures $T > 4$ K with a maximum at around 11 K revealing non-Debye behaviour. The temperature of this maximum corresponds to an energy of about 5–6 meV in the PDOS, i.e. to the energy range of the excess over a Debye law in the generalized PDOS.

This qualitative agreement suggests that the anomalous specific heat behaviour observed experimentally at around 12 K originates from the PDOS exceeding a Debye-like behaviour (similar to the case of $(TaSe_4)_2I$; see [18]).

The difference in absolute value from the experimental data from Odin *et al* [9] may be explained by the influence of the neutron weight $\sigma_i/m_i$ for each atom $i$ (see table 1) included in the generalized PDOS (see equation (4)), enhancing some features in the PDOS, and depressing others. Secondly, the difference is due to the fact that the specific heat curve for the lower temperature is very sensitive to the precise shape of the experimental PDOS, which is least reliable in the lowest 1 or 2 meV due to, in particular, uncorrected multiple-scattering processes.

### *3.2. $K_{0.3}MoO_3$: phonon dispersion and the low-temperature specific heat*

Figure 9 shows the low-energy phonon dispersion curves measured by Pouget *et al* [3]. They observed several acoustic and low-energy optic phonon branches along the two main directions of the system, the chain direction $[0, 1, 0]$ (within the $MoO_6$ sheets) and the direction $[2, 0, \bar{1}]$ (perpendicular to the $MoO_6$ layers), and along the corresponding boundaries of the Brillouin zone. The acoustic branches follow a sine-like dispersion except for the branch labelled '$LA_1$' that anti-crosses a low-lying optic branch (between 6 and 8.5 meV). For easier calculation we suppose this acoustic branch to be of sine-shaped dispersion (up to about 13.6 meV). The optic branch is approximated by the relation $\omega(q) = \omega_0 - aq^3$.

Since the experimental dispersion data (figure 9) are available for only *two* directions of the system, the low-energy PDOS is calculated for a model of cylindrical symmetry using the corresponding Christoffel equations. This simplification seems reasonable because of the sheet-like structure of the compound $K_{0.3}MoO_3$ (compare figure 3). In this model the potassium atoms play the role of atoms intercalated between two planes of $MoO_6$. The Kohn anomaly, also shown in figure 9, is omitted in the model calculation in order to include only phonon contributions to the PDOS coming from the 'normal' lattice dynamics, independently of the dynamics due to the Peierls transition.

Based on the symmetry of a system, the Christoffel equations relate the strain tensor **S** to the stress tensor **T** for acoustic lattice vibrations with small amplitude—that is, within the limit of Hooke's law. For a system of cylindrical symmetry this leads to the following equations [25]:

$$\begin{bmatrix} c_{11}k_x^2 + c_{66}k_y^2 + c_{44}k_z^2 & (c_{12} + c_{66})k_xk_y & (c_{13} + c_{44})k_xk_z \\ (c_{12} + c_{66})k_xk_y & c_{66}k_x^2 + c_{11}k_y^2 + c_{44}k_z^2 & (c_{13} + c_{44})k_yk_z \\ (c_{13} + c_{44})k_xk_z & (c_{13} + c_{44})k_yk_z & c_{44}k_x^2 + c_{44}k_y^2 + c_{33}k_z^2 \end{bmatrix} \begin{bmatrix} v_x \\ v_y \\ v_z \end{bmatrix}$$

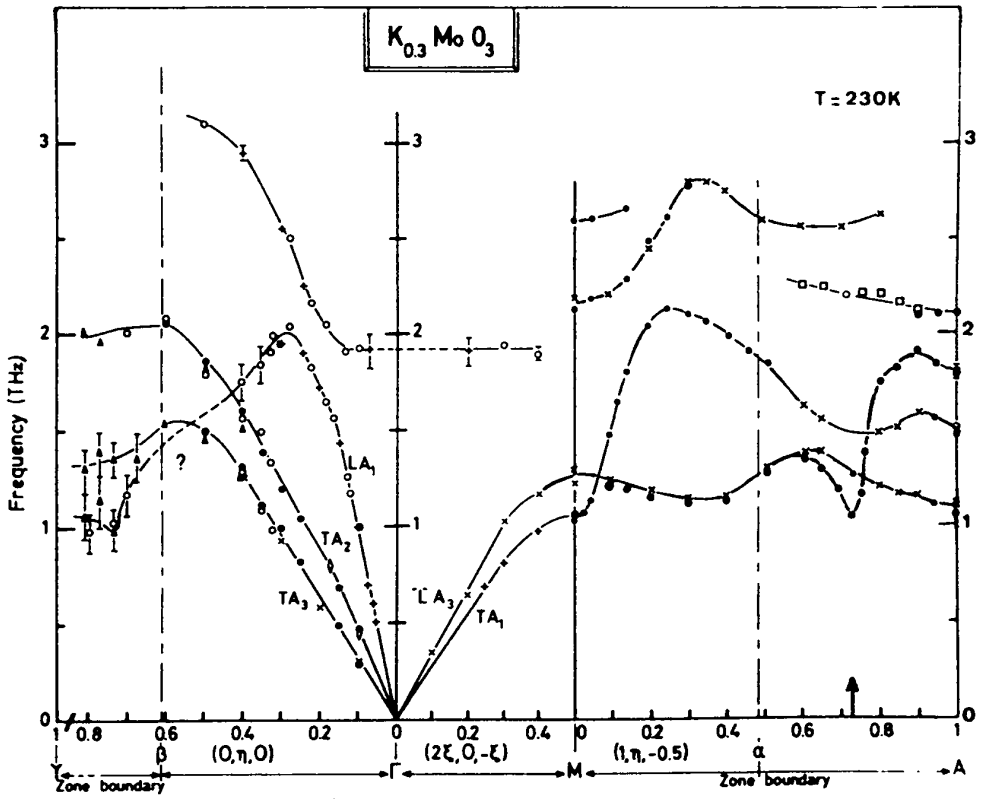


**Figure 9.** The dispersion of some low-energy phonon branches of the blue bronze $K_{0.3}MoO_3$ at a temperature of 230 K. The arrow indicates the Kohn anomaly. (This figure is taken from [3].)

$$= \rho\omega^2 \begin{bmatrix} v_x \\ v_y \\ v_z \end{bmatrix} \tag{6}$$

with the additional condition:

$$c_{66} = \frac{1}{2}(c_{11} - c_{12}).$$

The vector $\boldsymbol{v} = (v_x, v_y, v_z)$ denotes the polarization direction of the lattice vibration having the wave vector $\boldsymbol{k} = (k_x, k_y, k_z)$. When solving this vector equation one obtains a set of three equations of the type

$$\omega = A(c_{11}, c_{12}, c_{13}, c_{33}, c_{44})k \tag{7}$$

including the different polarization directions, which describe the behaviour of the acoustic phonon branches in the reciprocal space. The five independent coefficients $c_{ij}$ contained in these equations can be extracted from the sound velocities of the acoustic phonon branches. To introduce the sine-like phonon dispersion into the linear equations (7), $k$ is replaced by the expression

$$q_{ZB} \sin\left(\frac{\pi}{2}\frac{k}{q_{ZB}}\right)$$

with $q_{ZB}$ being the wavenumber at the zone boundary.

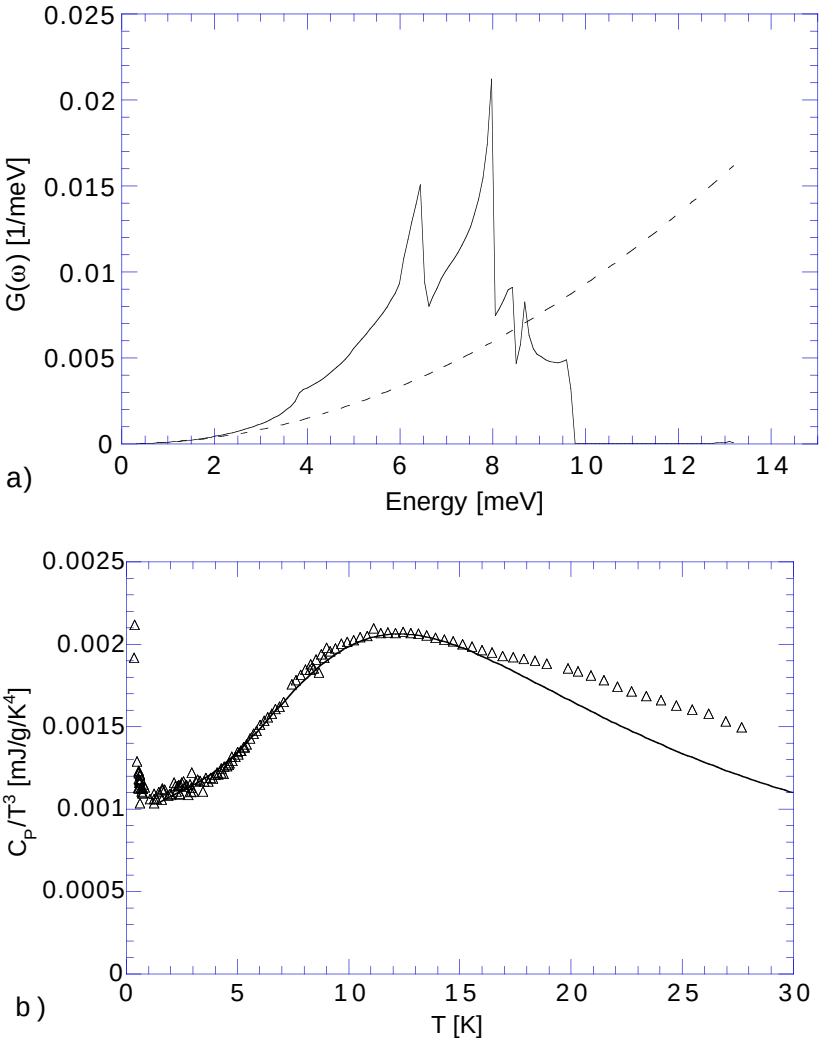


**Figure 10.** (a) The low-energy PDOS of $K_{0.3}MoO_3$ calculated from the simplified phonon dispersion model (see the text) (full line). The model PDOS is not convoluted with an instrumental energy-resolution function. The dashed line extrapolates the Debye law (see the text) to show the excess over a Debye behaviour. (b) The specific heat calculated from the model PDOS (full line). The model PDOS contains an adjustable factor, chosen to match the Debye parts of the calculated and the measured specific heat (see the text). The symbols show the experimental specific heat.

Figure 10(a) shows the low-energy PDOS, obtained from the simplified model described above. The PDOS is normalized so that when calculating the specific heat, the Debye plateau for the lowest few degrees Kelvin of the calculated $C_P/T^3$ matches that of the experimental specific heat data. This normalization offers the *only* adjustable factor in the whole calculation and, being only a scaling factor, does not quantitatively affect the excess of the PDOS over a Debye behaviour. The corresponding Debye law ($\omega_D = 31.8$ meV) is extrapolated to show the excess over a Debye behaviour of this calculated PDOS in an energy range between 4 meV and 8 meV. This excess is due to the PDOS contributions

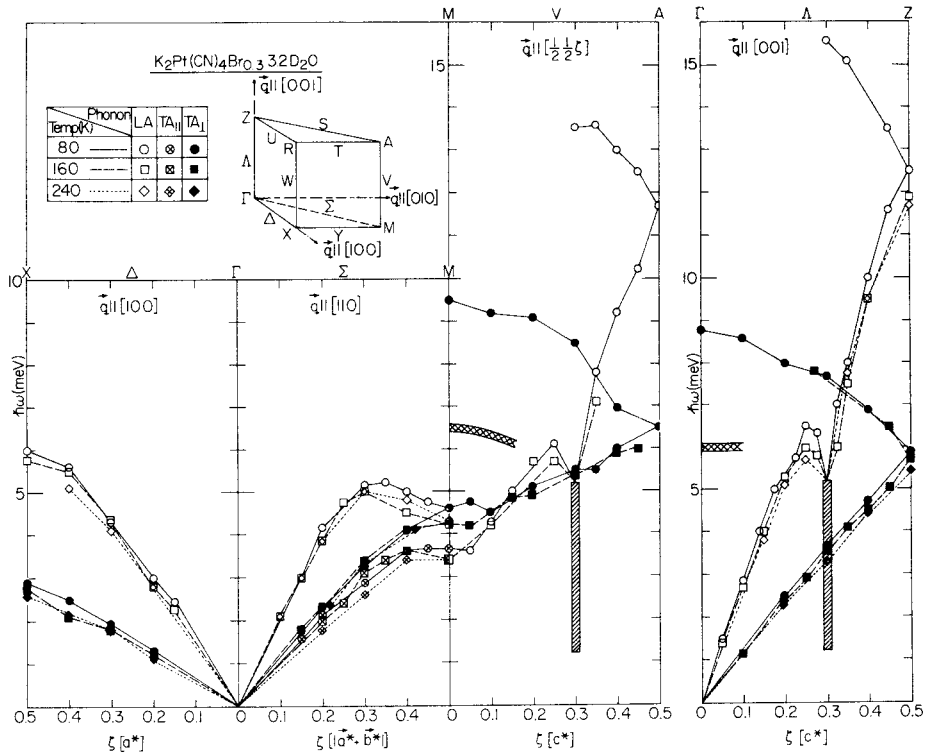


**Figure 11.** Phonon dispersion relations for deuterated KCP(Br) measured at the temperatures $T = 80$ K, 160 K and 240 K. The inset shows the irreducible part of the Brillouin zone and the assignments of the modes, where the symbols $\parallel$ and $\perp$ refer to the polarization being parallel or perpendicular to the chain axis $c^*$, [0, 0, 1]. The shaded areas correspond to $q_z = 2k_F$, where the wave-vector dependence of the scattering cannot be resolved. The cross-hatched areas show the position of the weak scattering that may correspond to an optic phonon. (This figure was taken from [5].)

from the longitudinal acoustic (LA) and transverse acoustic (TA) phonon branches, labelled '$TA_1$' and '$LA_3$', '$TA_3$' (see figure 9) together with the contribution from the low-lying optic phonon branch. The acoustic branches are flat at the zone boundary, therefore enhancing the phonon density of states between about 4 meV and 6.5 meV. The particular dispersion of the branch '$LA_1$' with its anti-crossing with the low-$\omega$ optic branch covers twice the energy range between 6 meV and 8.5 meV adding a strong contribution to the phonon density of states in this small energy range.

The specific heat calculated from the model PDOS is shown in figure 10(b). Despite the simplifications of the phonon dispersion introduced into the PDOS calculations, the model PDOS succeeds in reproducing very well the bump in the specific heat $C_P/T^3$ up to a temperature of about 15 K. The width of this bump is not reproduced because of the limited energy range (up to 9 meV) of the model containing only the acoustic branches and a contribution of the lowest optic phonon branch. Features at higher energies, like the structures visible in the generalized PDOS in figure 7, would contribute to the deviation of the specific heat from a Debye behaviour at temperatures above 15 K. In the model PDOS these features should certainly arise on considering further optic

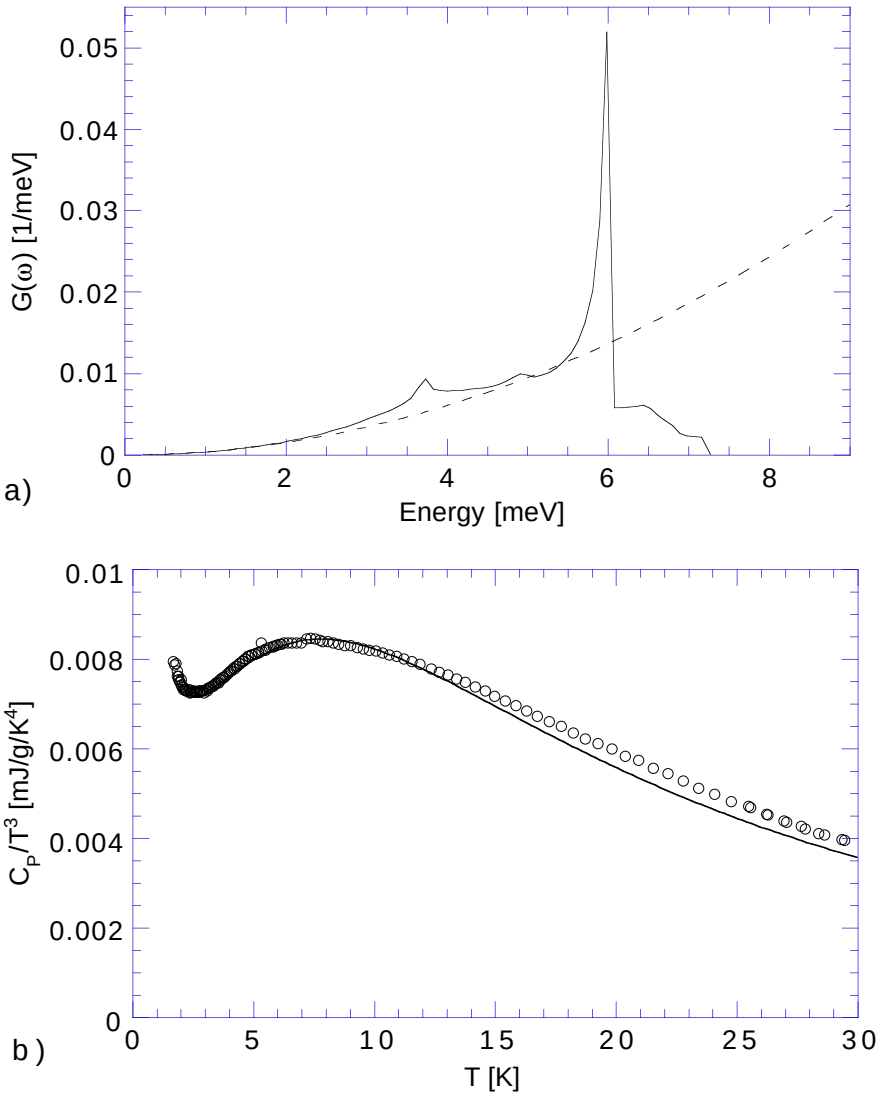


**Figure 12.** (a) The low-energy PDOS (full line) of deuterated KCP(Br) calculated from the phonon dispersion curves (see figure 11), including a low-lying optic branch at around 6 meV (see the text). The corresponding Debye law (dashed line) illustrates the excess of the PDOS over a Debye behaviour. (b) The specific heat $C_P/T^3$ (full line) calculated from the low-energy PDOS. The model PDOS contains an adjustable factor, chosen to match the Debye parts of the calculated and the measured specific heat (see the text). The experimental specific heat data are shown as symbols.

phonon branches and lead to an appropriate broadening of the deviation in the calculated $C_P/T^3$.

### *3.3. KCP: phonon dispersion and the low-temperature specific heat*

On the basis of the available phonon dispersion curves measured for deuterated KCP(Br) [5] we have performed calculations of the low-energy PDOS; this is similar to the approach that is used for $K_{0.3}MoO_3$. Figure 11 shows the low-energy phonon branches, observed along the three principal directions [1, 0, 0], [1, 1, 0] and [0, 0, 1] of the tetragonal system. Several acoustic branches show a basically sinusoidal dispersion, such as the LA branch propagating along [1, 0, 0] and the TA branches along [1, 1, 0], whereas others behave rather linearly, like the TA branch along [1, 0, 0]. The acoustic branches propagating along [0, 0, 1] can be taken as sinusoidal in an extended zone scheme along the chain direction $c^*$. As for the blue bronze, the Kohn anomaly at around $0.3c^*$ is omitted for the calculation of the PDOS.

Like the branch '$LA_1$' of $K_{0.3}MoO_3$ (see figure 9), the longitudinal acoustic branch along [1, 1, 0] for KCP deviates significantly from a simple sinusoidal or linear dispersion. This deviation suggests an anti-crossing with a low-energy optic phonon branch (lying between about 5 and 7 meV). In fact, the observed phonon dispersion of KCP(Br) (figure 11) shows parts of an optic phonon branch at around 6–6.5 meV observed close to the $\Gamma$ point and to the M point of the Brillouin zone. To include this optic branch in the calculation of the PDOS these two branches are approximated as an acoustic branch with sine-like dispersion crossing an optic branch estimated again to be of the type $\omega(q) = \omega_0 - aq^3$.

The calculation of the low-energy PDOS of KCP(Br), up to an energy of about 7 meV, is performed using the Christoffel equations for the symmetry class $4mm$ (see Auld [25]). These equations are based also on equation (6) but with no additional condition for the coefficient $c_{66}$. Similarly to the case of the blue bronze, the independent coefficients $c_{ij}$ ($c_{11}, c_{12}, c_{13}, c_{33}, c_{44}$ and $c_{66}$) of the Christoffel equations are determined from the sound velocities of the different acoustic phonon branches.

Figure 12 shows the calculated low-energy PDOS, normalized so that the slope of the Debye part (up to about 1 meV) leads to a matching between the Debye plateaus of the calculated and the experimental specific heat. In the figure the corresponding Debye law (with $\omega_D = 19.9$ meV) is extrapolated to show the excess of the PDOS over a Debye behaviour between about 2.5 meV and 6 meV.

From the calculation, the excess at energies up to about 4 meV is due to the PDOS contribution of the TA branches polarized perpendicularly to the direction of the platinum chains, [0, 0, 1], and among them mainly the TA branch propagating along [1, 1, 0]. The excess at around 5–6 meV originates from the contribution of the estimated low-energy optic branch. As for the case of $K_{0.3}MoO_3$, the slope of the Debye law is used as the (only) adjustable parameter to match the Debye part of the calculated and the experimental specific heat data.

Calculating the specific heat from the model PDOS obtained for KCP reveals a bump in $C_P/T^3$ centred at around $T = 7.5$ K in very good agreement with the experimental data up to a temperature of about 13 K, as shown in figure 12. As for $K_{0.3}MoO_3$, the deviation of the calculated from the experimental values for the higher temperatures is due to the limited energy range of the calculated model PDOS (up to about 7 meV).

## 4. Conclusion

We have studied the origin of the deviation of the specific heat from a Debye behaviour, the $C_P$-'anomaly', observed in the blue bronze ($T_{anom} = 12$ K) and KCP(Br) ($T_{anom} = 7.5$ K) by extracting the generalized PDOS (for the blue bronze) from time-of-flight measurements

and by a calculation of the low-energy PDOSs. The generalized PDOS of $K_{0.3}MoO_3$ reveals an excess over a Debye behaviour, which leads to an 'anomaly' in $C_P$ centred at around $T_{anom}$ ($\approx$12 K). From the results of the calculations presented in sections 3.2 and 3.3 for $K_{0.3}MoO_3$ and KCP, respectively, we have found a very good agreement between the calculated and the experimental specific heat data. Since the model PDOSs are calculated by omitting the dynamics related to the Peierls transition (Kohn anomaly, phasons), the model PDOSs contain *only* contributions from 'normal' lattice phonons. With these results one can establish a lattice phonon origin of the anomalous specific heat behaviour observed at around 12 K and 7.5 K for the blue bronze $K_{0.3}MoO_3$ and KCP(Br), respectively, corresponding to the basic idea of Konate [8].

As shown by the model calculations and differing from Konate's interpretation, the observed 'anomalies' of the specific heat are built up partially from PDOS contributions from flat sections of *acoustic branches* near the Brillouin-zone boundary *as well as* an important contribution from a *low-energy optic branch*.

In the particular case of $(TaSe_4)_2I$, the low-energy optic branch observed at around 4.2 meV does not play any role for the observed specific heat behaviour. If it did, the corresponding contribution to the specific heat would be observable near about 9 K, whereas the observed bump in $C_P/T^3$ is at around 1.8 K. Compared to the blue bronze and KCP, the compound $(TaSe_4)_2I$ appears to be somewhat unusual due to the existence of the nearly dispersionless, very low-lying ($\approx$0.7 meV), transverse acoustic branch propagating perpendicularly to the chain direction. It is only this particularly flat acoustic branch which gives rise to the specific heat behaviour of $(TaSe_4)_2I$. This flat, low-lying branch shows a low sound velocity leading to a steep slope of the Debye behaviour within the first 1 meV.

Since the anomalous specific heat behaviour observed in the three CDW systems $(TaSe_4)_2I$, KCP and the blue bronze $K_{0.3}MoO_3$ is not due to properties related to the Peierls transition but to 'normal' lattice dynamics, it should be observable also in *non*-CDW systems. In fact, similar specific heat 'anomalies' at temperatures around 10–20 K have been observed for the quasi-one-dimensional superconductors $M_2Mo_6Se_6$ (M = Tl, In, Rb, Cs) by Bonjour *et al* [26]. These $C_P$-'anomalies' have been related to Einstein-like phonon modes corresponding to optical vibrations of the M atoms at energies between 6 meV and 10 meV contributing to the PDOS of these compounds ([26] and Brusetti *et al* [27]). So, for the compounds $M_2Mo_6Se_6$ as well, a low-energy optic branch plays an important—even the principal—role in the lattice phonon origin of the observed specific heat behaviour, like for the compounds blue bronze and KCP studied here.

In contrast to these structurally rather complicated, (quasi-) low-dimensional systems, similar specific heat 'anomalies' of lattice phonon origin have been found in diamond-type semiconductors [28], like germanium [29], and in cristobalite [30]. For these systems the specific heat behaviours have been related to flat transverse acoustic phonon branches.

A question not touched in this work concerns the relation between the phonon branches giving rise to the specific heat behaviour and the kinds of atom and their corresponding displacements. Here, further studies, e.g. following the scheme of the study of the $M_2Mo_6Se_6$ compounds (M = Tl, In, Rb, Cs), are certainly required, combining measurements of the specific heat, the phonon density of states and, additionally, the phonon dispersion curves.

## Acknowledgments

The authors acknowledge useful discussions with H Schober. We thank K Biljaković, J Odin and K Hasselbach for providing us with their specific heat data on $K_{0.3}MoO_3$.

H Requardt acknowledges the financial support of an 'Allocation de Recherche' from the French Ministry of Education and Research (MESR).

## References

[1] Grüner G 1994 Density waves in solids *Frontiers in Physics* vol 89 (New York: Addison Wesley)
[2] *ECRYS '93* 1993 *J. Physique (JPI Suppl.)* I **3** 215
[3] Pouget J P, Hennion B, Escribe-Filippini C and Sato M 1991 *Phys. Rev.* B **43** 8421
[4] Pouget J P, Hennion B and Sato M 1993 *J. Physique Coll. (JPI Suppl.)* IV **3** 215
[5] Carneiro K, Shirane G, Werner S A and Kaiser S 1976 *Phys. Rev.* B **13** 4256 and references therein
[6] Lorenzo Diaz J E 1992 *PhD Thesis* Grenoble University, France
[7] Biljaković K, Lasjaunias J C, Zougmore F, Monceau P, Levy F, Bernard L and Currat R 1986 *Phys. Rev. Lett.* **57** 1907
[8] Konate K 1984 *PhD Thesis* Grenoble University, France
[9] Odin J, Biljaković K, Hasselbach K and Lasjaunias J C 1997 to be published
[10] Odin J, Lasjaunias J C, Berton A, Monceau P and Biljaković K 1992 *Phys. Rev*. B **46** 1326
[11] Donovan S, Kim Y, Alavi B, Degiorgi L and Grüner G 1990 *Solid State Commun.* **75** 721
[12] Kim T W, Reagor D, Grüner G, Maki K and Virosztek A 1989 *Phys. Rev.* B **40** 5372
[13] Monceau P, Bernard L, Currat R, Levy F and Rouxel J 1986 *Physica* B **136** 352
[14] Brown S E, Willis J O, Alavi B and Grüner G 1988 *Phys. Rev.* B **37** 6551
[15] Kim Tae Wan, Donovan S, Grüner G and Philipp A 1991 *Phys. Rev*. B **43** 6315
[16] Biljaković K, Lasjaunias J C and Monceau P 1991 *Phys. Rev.* B **43** 3117
[17] Biljaković K, Lasjaunias J C and Monceau P 1989 *Synth. Met.* **29** F289
[18] Lorenzo J E, Currat R, Dianoux A J, Monceau P and Levy F 1996 *Phys. Rev*. B **53** 8316
[19] Degiorgi L, Alavi B, Mihály G and Grüner G 1991 *Phys. Rev.* B **44** 7808
[20] Graham J and Wadsley A D 1966 *Acta Crystallogr*. **20** 93
[21] For a review on bronzes see
Schlenker C (ed) 1989 *Low-dimensional Electronic Properties of Molybdenum Bronzes and Oxides* (Dordrecht: Kluwer Academic)
[22] For a review on platinum chain compounds see
Carneiro K 1985 Properties of conducting platinum chain compounds *Electronic Properties of Inorganic Quasi-one-dimensional Materials* vol 2, ed P Monceau (Dordrecht: Reidel)
[23] Heger G, Deiseroth H J and Schulz H 1978 *Acta Crystallogr*. B **34** 725
[24] Egelstaff P A and Schofield P 1962 *Nucl. Sci. Eng.* **12** 260
[25] Auld B A 1973 *Acoustic Fields and Waves in Solids* vol 1 (New York: Wiley)
[26] Bonjour E, Calemczuk R, Khoder A F, Gougeon P, Potel M and Sergent M 1985 *Proc. 2nd Int. Conf. on Phonon Physics (Budapest)* (Singapore: World Scientific) p 750
[27] Brusetti R, Dianoux A J, Gougeon P, Potel M, Bonjour E and Calemczuk R 1990 *Phys. Rev.* B **41** 6315
[28] Weber W 1974 *Phys. Rev. Lett.* **33** 371
[29] King C N, Phillips W A and deNeufville J P 1974 *Phys. Rev. Lett* **32** 538
[30] Bilir N and Phillips W A 1975 *Phil. Mag.* **32** 113